Journal of the Korean Ceramic Society
Vol. 45, No. 7, pp. 380~386, 2008.

Nanoparticle Phosphors Synthesized by Inductively Controlled Plasma Process for Plasma Based Display

Choong Jin Yang†, Jong-Il Park, Seung Dueg Choi, Eon Byeong Park, and Young Joo Lee

Nanotechnology Research Labratory, Research Institute of Industrial Science & Technology(RIST), Pohang 790-330, Korea
(Received May 8, 2008; Accepted July 23, 2008)

ABSTRACT

Optimized volume production of nanoscale phosphor powders synthesized by radio frequency (RF) plasma process was developed for the application to plasma display panels. The nano powders were synthesized by feeding the both solid and liquid type precursors, and nanoparticle phosphors were characterized in terms of particle size, shape, and photoluminescence (PL) intensities. Computer simulation was performed in advance to determine the process parameters, and nano phosphors were evaluated by comparing with current commercial micron-sized phosphor powders. Practical feeding of both solid and liquid type precursor was proved to be effective for volume production.The developed process showed a potential as a production method for red, blue and green phosphor although the PL intensity still needs further improvement.

Key words **: *Nanoscale phosphor, RF plasma, Plasma display panel, PL intensity***

1. Introduction

A cost-effective production process for display materials requires a strong problem-solving approach for current PDP and LCD sectors. Sooner or later, the roll to roll, and ink jet printing will be adopted as a basic electronic printing technology. Accordingly the nanoscale powder precursors which are essential for the printable electronics inks will become more important in the near future. The present study was focused on nanoscale phosphor powders applicable to digitally printable inks or pastes for display panels. The powder shape and size, size distribution, photoluminance and production process are critical issues for this promising portion of the new and emerging display market. Therefore, the present study focuses on the development of an optimized production process of nanoscale phosphors having potential characteristics comparable to commercial micron-sized powders.

1.1. RF plasma as a heat source and chemical reaction

Thermal plasmas are mainly generated in DC arc and RF induction torches. RF plasma compared to DC arc discharge has some advantages. As a heat source, the plasma can be inductively heated by radio-frequency-generated power of many tens of kW or even several MHz.[1-2] From an engineering perspective, the torch can be designed to generate a region of plasma volume about 30~40 cm in diameter. The axial velocity as a chemical reaction source is as low as 10 m/sec, the residence time of plasma flame at high temperature is as long as tens of milliseconds, which is very useful for chemical reactions to process nanoparticle synthesis. Since during the generation of RF induction plasma any kind of gas can be used to generate the plasma gas, this thermal plasma provides the chemical reaction for various metals and their oxides in a spherical shape of nanoscale.[3-5]

1.2. Nanoparticles synthesis in RF plasmas

In a high temperature thermal plasma highly crystalline nanoscale particles of metals and their oxides with exact spherical shapes can be produced. With this process it is possible to control the sizes and phase compositions of oxides or any other compounds using one-step in-flight oxidation when solid type precursors are fed into the reaction chamber. The fed powder precursors are melted in the high temperature plasma and simultaneously oxidized. Then in some cases the increased vapor pressure gives rise to a relatively high degree of supersaturation in the vapor phase or phases. By flying far away from the heat source those phases are cooled and condensed to from spherical and crystalline metal or oxide particles with sizes on a nanometer to submicrometer scale.[6-7] The use of a solid type precursor, however, often causes the problems of wide ranging particle size distribution.

In order to solve the problems mentioned above liquid precursors such as suspension type or solution type precursors are being used as well.[8] In these processes the precursor liquid is fed into the atomizing nozzle and misted into atomized droplets through the nozzle tip. Of course the carrier gas, Ar, should be blown through the nozzle as in the process for solid precursors. Suppose a mist of a droplet size

†Corresponding author : Choong Jin Yang
E-mail : cjyang@rist.re.kr
Tel : +82-54-279-6331 Fax : +82-54-279-6629

having 10~50 micrometers is fed into a plasma reactor, the mist vaporizes instantaneously enabling a massive reaction to take place into nanoparticles in the reactor space. In general chemical compositions of nano oxide particles, for instance, can be adjusted with the prepared cation ratios of precursor liquid, and process parameters in the synthesis of those oxides can be adjusted by precise flow control of Ar, and O_2 gases and RF power intensity. Since size control is crucial for those nanoparticles considering the functions of application area, narrowing the size distribution of the nano process using liquid type precursor enables the plasma process to be extended into further industrial applications.

2. Experimental Procedures

The properties of current commercial PDP phosphors of red(YBO_3), green(Zn_2SiO_4), and blue ($BaMgAl_{10}O_{17}$) were bench-marked for the development of nano phosphors in terms of powder size, shape, and PL intensity taking into account process availability. Basically, solid precursor powders were prepared via conventional solid reaction followed by ball milling before feeding them into the RF plasma reactor. The powder sizes of each precursor were 10~50 micrometer. In this study the development of a feeding technique of the precursor was focused which is classified into two methods, i.e., solid precursor and liquid precursor. For the present plasma process, (a) dry precursor of milled powder was fed into the reactor where the inlet powders were vaporized and then condensed into nano particles of phosphor having the required composition. Controlling the stoichiometric composition and doping element was a key technology. In some necessary cases, the synthesized nano phosphors were immersed into a solution containing the doping element followed by additional heat treatment to compensate for dopant lost during nano synthesis. (b) Feeding either the suspension or solution precursor containing the blended elements into the reactor directly was also performed. In this case an elaborated post heat treatment was essential to improve the inferior properties of PL intensity compared to case (a). Production yield must be improved for commercial volume production. Photoluminescence (PL) spectra were measured with a spectrofluorometer (Kontrom SFM 25) which is composed of a 150 W Xe high pressure arc lamp, two monochromators (1200 line/nm; f.l.=

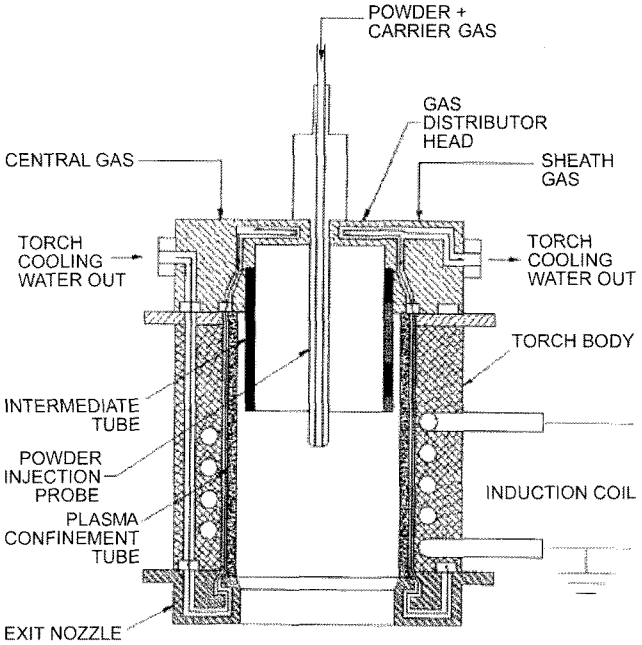

Fig. 1. RF plasma nozzle used for the simulation and nano synthesis of Phosphor powders in this study.

100 nm, $D^{-1}=8$ nm/mm, and a photomultiplier tube (PMT Haramatsu R 928).

3. Results and Discussion

3.1. Computer simulation of plasma combustion

As mentioned already nucleation from gas phase and subsequent particle growth took place in the tail section of plasma flame. Therefore, size control had to be performed by controlling the temperature profile and stream profile of hot plasma gas. For the nanoparticle synthesis of oxide species in this study, the temperature and gas stream profiles were simulated in advance by varying the levels of carrier Ar, sheathing O_2, and central Ar gas, and at the same time using the injection nozzle as shown in Fig. 1. For the computer simulation of mathematical modeling, the following basic assumptions were proposed, axisymetric-two dimensional system of coordinates, steady state laminar or turbulent flow, plasma in local thermodynamic equilibrium, optically thin plasma, property fluctuations in the turbulent

Table 1. Process Parameters of RF Plasma Used in the Simulation

Case No	Operating conditions							
	Powder feed rate (g/min)	Reactor pressure (kPa)	Powder carrier gas Ar, He (slpm)	Sheath O_2 (slpm)	Sheath Ar (slpm)	Central Ar (slpm)	Gauge power (kW)	Probe (id.4,5 mm) position (cm)
1	0	50	5 Ar	12,5	90	30	65	Center of 5-turn coil
2	0	50	10 Ar	12,5	90	30	65	
3	0	50	10 He	12,5	90	30	65	
4	0	50	10 He	25,0	90	30	65	
5	0	120	10 He	25,0	90	30	65	

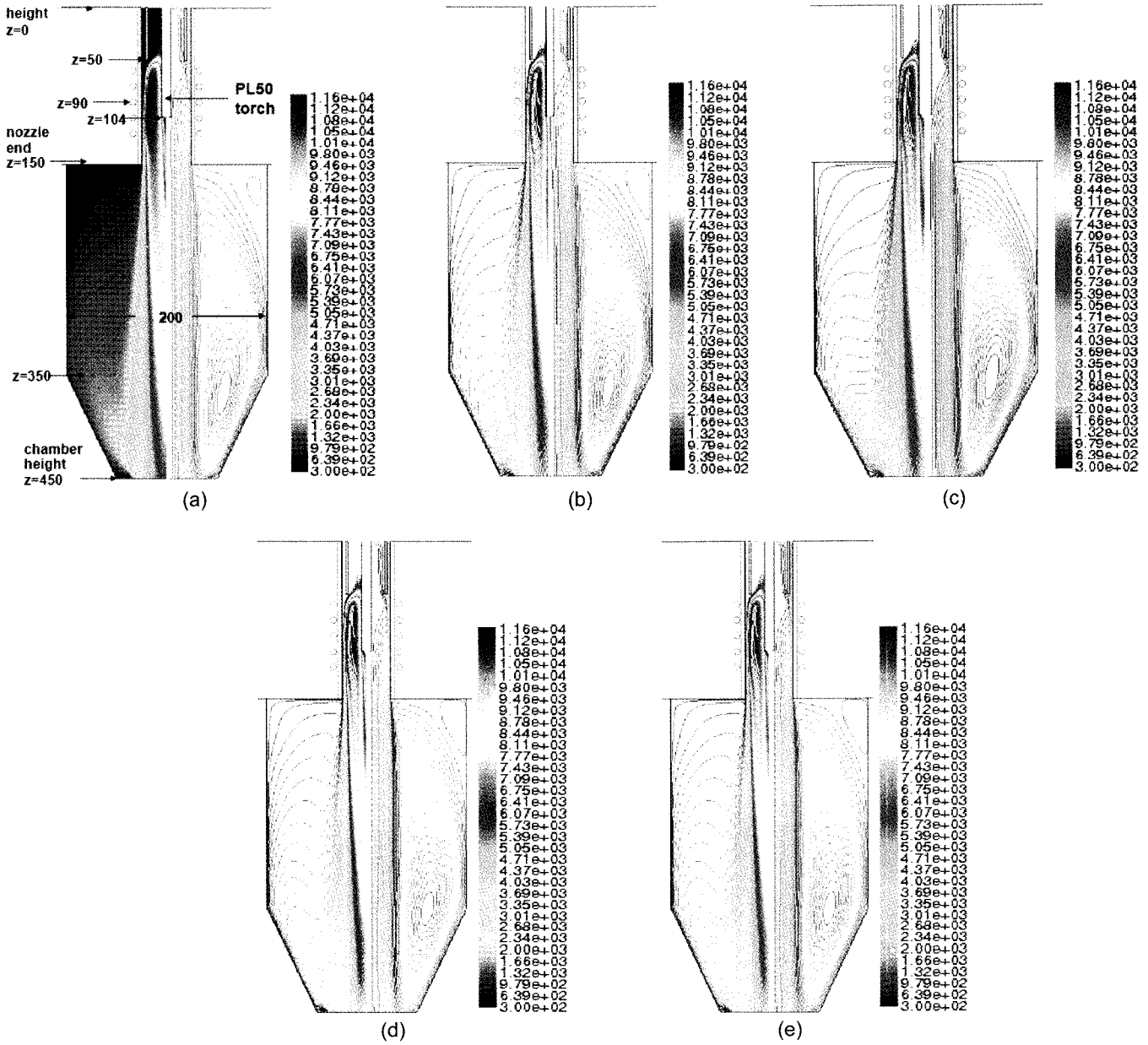

Fig. 2. (a) Temperature profile(left hand column) and stream function profile (right hand column) of the Case 1 study, (b) Temperature profile(left hand column) and stream function profile (right hand column) of the Case 2 study, (c) Temperature profile(left hand column) and stream function profile (right hand column) of the Case 3 study, (d) Temperature profile(left hand column) and stream function profile (right hand column) of the Case 4 study, and (e)Temperature profile(left hand column) and stream function profile (right hand column) of the Case 5 study.

flow case limited to the density, negligible viscous dissipation of kinetic energy. The mathematical modeling was done by governing the equations of continuity, momentum, thermal energy, mass transfer, kinetic energy, and vector potential for the electromagnetic field of the reactor system. Table 1 shows the process parameters used in simulating the RF plasma reaction in the system. Figures from 2(a) to 2(e) show the simulated profiles of temperature and stream functions. The numbers in iso-contours indicate the temperature in K. This simulation resulted from the assumption that the used power was only 60% of designed full power of 50 kW. Case 4A in Fig. 3 has the same conditions as Case 4 except that the power used was 40% of full power. The dimensions of the system used in this simulation are indicated in Fig. 2(a) for the reactor chamber and precursor injecting probe as well.

In general, Ar gas was being used during the real RF plasma process for the synthesis of nano powders of metals and their oxides. Fig. 3 shows little difference in the temperature profiles in the reactor chamber at the range of 250~400 cm high(z) from the inlet of precursor injection probe. Also every case study indicates an almost uniform

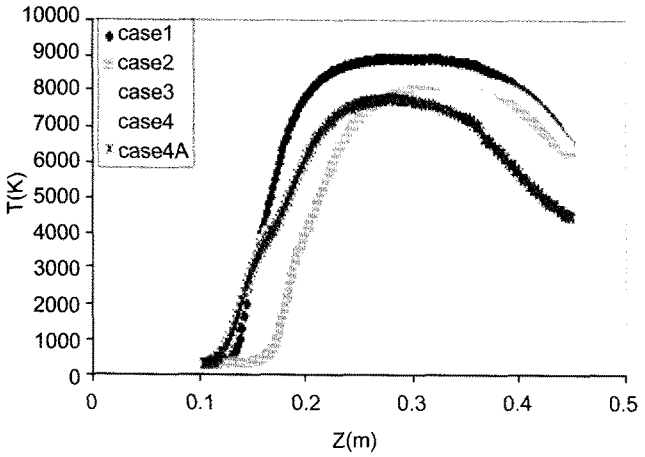

Fig. 3. Temperature profiles of cases studied by varying the process parameters Case 4A is same as Case 4 except for the efficiency of power supply being reduced from 65% to 40%.

plateau distribution at the height zone of 250~400 cm. However, the simulated results show a different the maximum temperature in that zone. The use of less carrier gas and/or sheath gas introduces a higher maximum temperature and the maximum obtained temperature is about 9000 K for the Case 1. Once the flow rate of carrier gas is doubled from 5 to 10 standard liters per minute as in Cases 2 and 3, the maximum temperature in the same zone looks to drop to about 8000 K as shown in Fig. 3. Likewise when carrier gas is changed from Ar to He, or the gas flow rate of sheath gas, O_2, is doubled from 12.5 to 25 standard liters per minute the maximum temperature in the same zone in the reactor chamber drops again to the 8000 K range. On the basis of this preliminary simulation the authors were able to proceed to the synthesis of nano phosphors.

3.2. Nano phosphors synthesized by feeding solid precursor

Fig. 4(a) shows nano green phosphors of Zn_2SiO_4:Mn made by feeding dry precursors. The precursors were prepared by solid reaction with perfect composition control and variation of Mn dopant from 5 to 12 at %, and followed by a conventional milling process to an average size of 40 micrometers. Basically, the solid reaction using ZnO, SiO_2 and $MnCO_3$ powders was carried out at 1200~1400°C to obtaine a stoichiometric Zn_2SiO_4 composition. However, ZnO and SiO_2 powders were well mixed with $MnSO_4$ which allows convenient and precise control of the desired dopant, Mn. Both cases showed the best stoichiometry when the ratio of Zn/Si was 1.6/1. After the nano synthesis, the precursor containing 12 at.% Mn exhibited appropriate properties after the heat treatment of annealing at 1200°C for 1 h under H_2 environment. Considering only PL intensity the synthesized nano phosphors exhibited an inferior brightness when compared to the commercial micron powders as shown in Fig. 4(b). However, the decay time of afterglow was found to be shortened very much by the effects of the nano process in terms of size and shape. Fig. 4(c) indicates the shortened decay time of nano phosphor, which was found in every synthesized phosphors at 528 nm(green), 453 nm(blue) and 610~615 nm(red) wavelengths in the spectra[9,10]. The reason may be that the nano phosphors have less surface defects than the particles made by conventional powder metallurgy. Nano synthesis enables the nanoparticles to have fewer crystallographic distortions as well as shallower trap level than that of phosphors prepared by solid reaction.[10] Therefore the relative intensity of afterglow is lowered and the decay of afterglow is shortened. This shortened decay time was more prominent when appropriate Li was doped as shown in Fig. 4(d). The figure shows the comparison of decay time for the samples of $Zn_{1.9}SiO_4$:$Mn_{0.05}Li_{0.05}$, $Zn_{1.9}SiO_4$:$Mn_{0.05}B_{0.05}$ and $Zn_{1.95}SiO_4$:$Mn_{0.05}$, respectively. The cross bar in the figure is the boundary indicating 20% of the initial intensity of 528 nm green rays. By doping Li together with Mn appropriately, the decay time was reduced to only 3 msec. Otherwise, green phosphor of virgin composition exhibited the decay time longer than 6 msec which is double that of Mn/Li co-doped. When only Mn was doped, the decay time was extended up to 13 msec, although the PL intensity was shown to increase greatly as shown in Fig. 4(e). In general, many defects may be dispersed on the surface of nano phosphors, which may result in a relatively lower amount of luminescent center Mn^{2+} in the Zn_2SiO_4 lattice available for direct radiation. Furthermore, with the addition of Li, high speed of hole mobility and electron-hole recombination between $^2T_2$ and $^5E_2$ status in nano phosphors with good crystallinity will decrease retrapping probability and further prompt the decay process.[11,12]

Nano blue phosphor of $BaMgAl_{10}O_{17}$:$Eu_{0.12}$ was synthesized by feeding the dry powders of average 40 micrometer size. Then appropriate proprietary heat treatment was carried out under H_2 environment at the temperatures from 900 to 1450°C for 1 h. The optimized PL intensities of every nano phosphors were hardly obtained right after synthesis. Heat treatment at high temperature above 1400°C helped the enhancement of PL intensity. After this treatment there was no change in shape or composition for BAM powders because the temperature range of about 1400°C is still low enough to prevent the powers from diffusive growth. Fig. 5(a) indicates the effect of heat treatment on the typical BAM blue nano phosphors, which show an enhanced PL intensity when temperature is varied from 1000 to 1400°C under H_2 environment. The optimized treatment resulted in almost 70% of the PL intensity of commercial BAM blue. The inferior properties of both nano green and blue phosphor were found to be enhanced approximately 60~70% by controlled doping of Li and Eu. X-ray pattern in Fig. 5(b) indicates the existence of minor phase $SiAl_2O_4$ which was present right after nano synthesis but finally disappeared after heat treatment above 1400°C.

RF plasma process was also employed in producing red nano phosphors of Y_2O_3;Eu and (YGd)BO_3:Eu. However, the

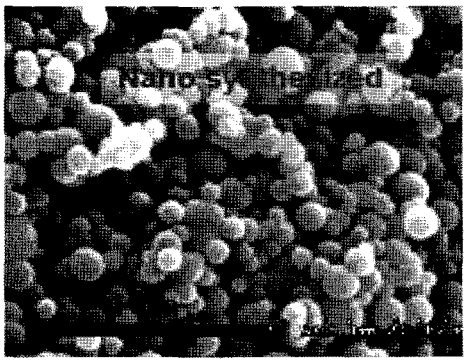

(a)

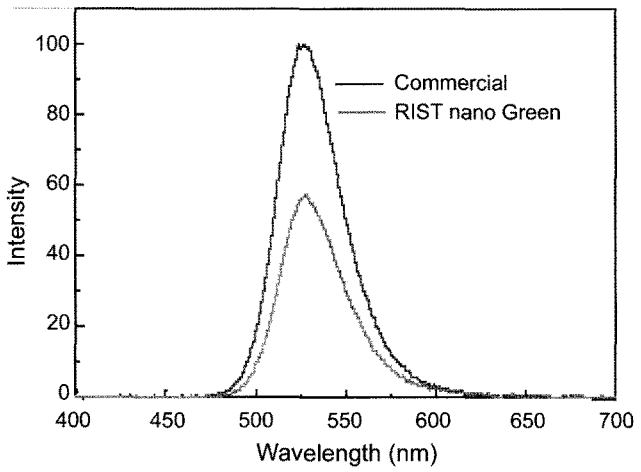

(b)

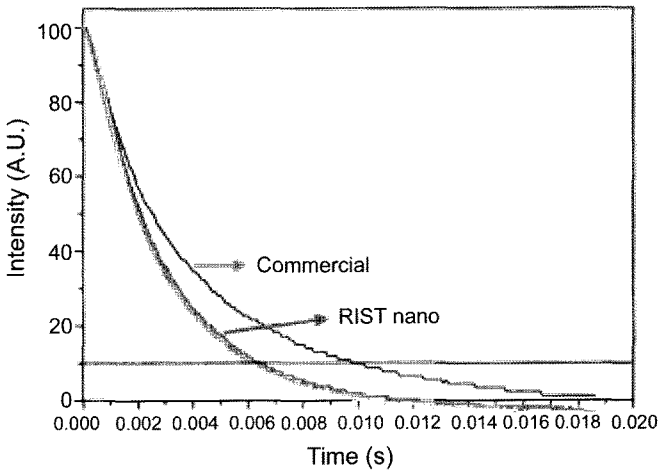

(c)

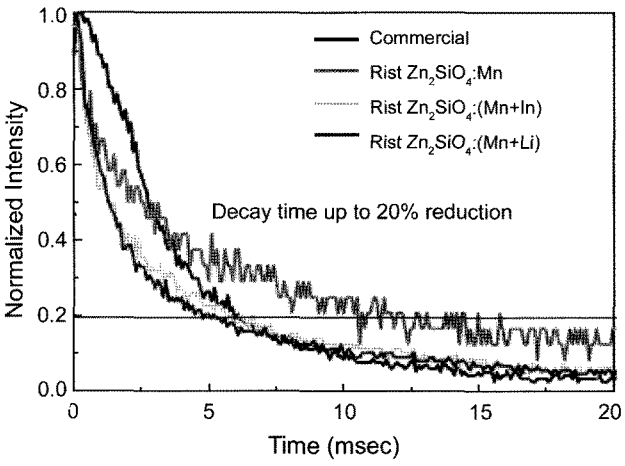

(d)

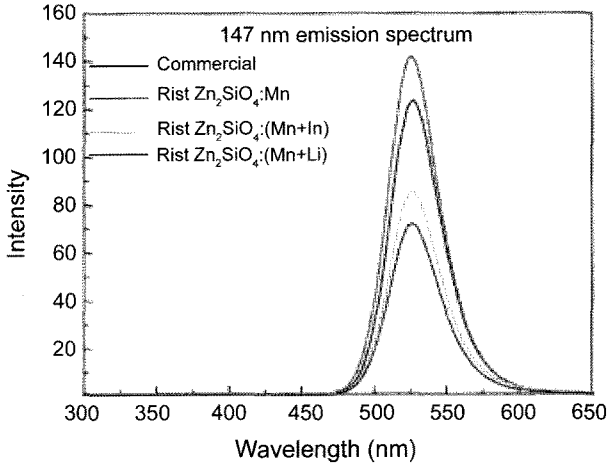

(e)

Fig. 4. (a) Nano green phosphor of Zn_2SiO_4 processed by feeding solid precursor, (b) Comparison of PL intensity measured at 147 nm emission spectra, (c) Nano green phosphors showing the shortened decay time by the effect of nano process, (d) Prominently shortened decay time by the addition of Li into Mn doped Zn_2SiO_4 nano green phosphors, and (e) The effect of Li and Mn doping on PL intensity compared with the commercial green phosphor of micrometer.

doping process of the activator, Eu, was pursued in various approaches. The most promising technology was one in which host materials were nano processed in size first and then dipped into Eu-nitrated solution, which was followed by an optimized heat treatment. Fig. 6 shows typical Y_2O_3:Eu nano red phosphor synthesized by feeding dry precursor and followed by dipping into Eu $(NO_3)_3$ solution, and then heated at 900°C for 2~3 h. This process enabled the host material to dope Eu up to 6.4 at. % which gave the highest PL intensity, as shown in Fig. 6. Processing the dry precur-

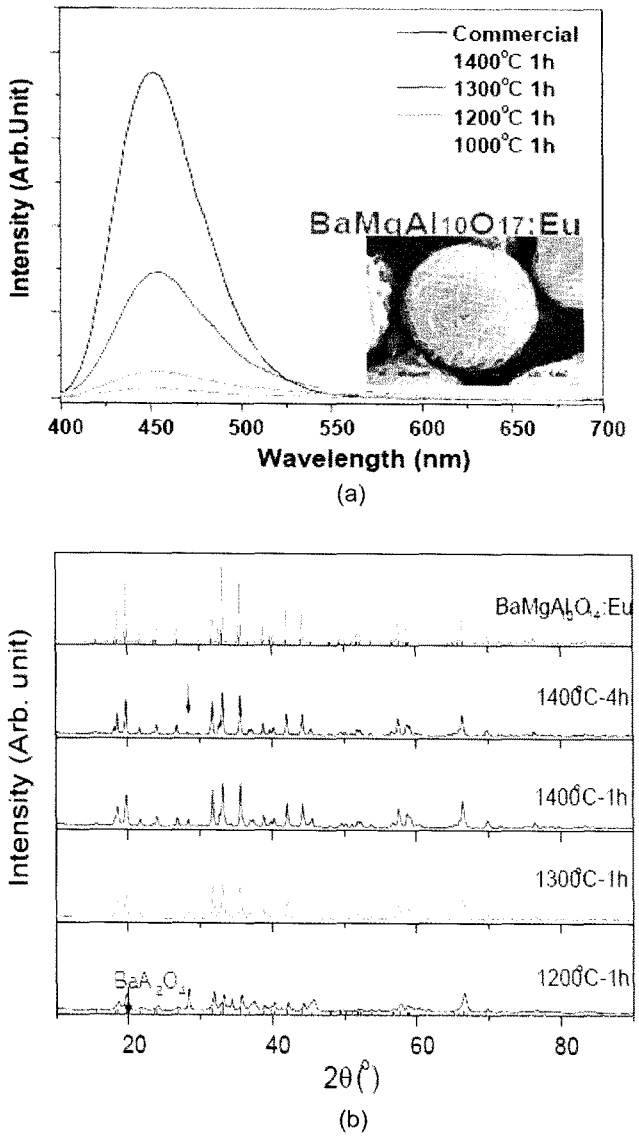

Fig. 5. (a) Enhanced PL intensity after heat treatment for the typical BAM nano blue phosphor, (b) Phase transformation of BAM nano blue phosphor during the heat treatment. Intermediate phase $BaAl_2O_4$ disappears(arrow in the inset) after the heat treatment at 1400°C.

sor into nano phosphors followed by an appropriate heat treatment is a promising route for RF plasma synthesis. However, the problem of inferior properties must be solved by developing a certain type of cycle of heat treatment, and optimized doping of activator. In general, the shape and size of nano powders synthesized from dry precursors show an excellent localized distribution, as can be seen in the TEM micrographs shown in Figs. 4(a), 5(a) and 6.

3.3. Nano phosphors synthesized by feeding liquid precursor

Two approaches were possible in producing nano phosphors by feeding liquid type precursors. One was to feed the precursor of suspension composing micron host powders

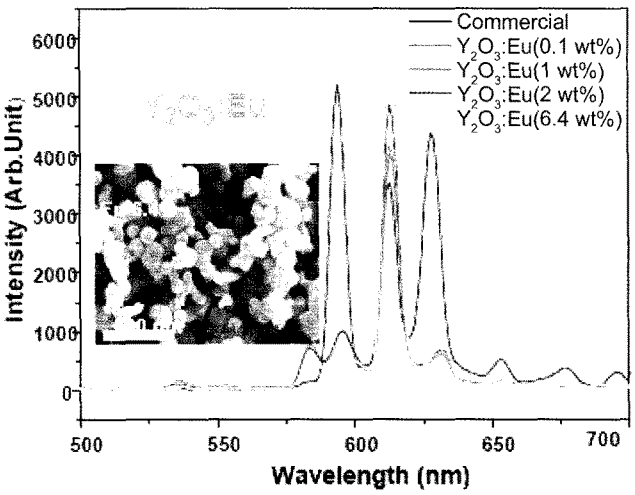

Fig. 6. Nano red phosphor of Y_2O_3 :Eu processed by feeding dry precursor

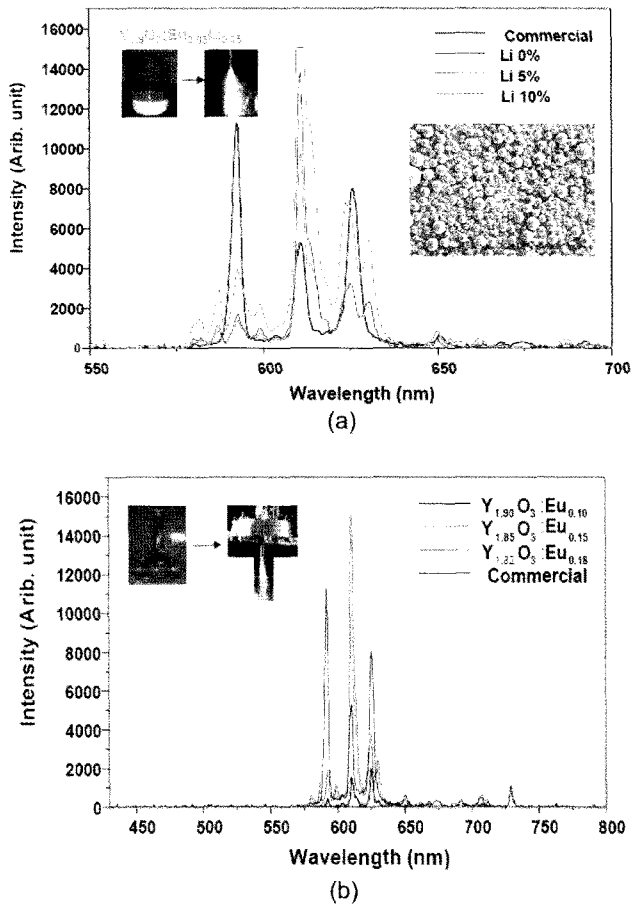

Fig. 7. (a) PL intensity of nano red of Y_2O_3:Eu processed by suspension precursor containing Li for enhanced properties, (b) PL intensity of nano red Y_2O_3:Eu processed by aerosol solution precursor.

into the salt of activator material. The other was to blend the salts of both materials. Figs. 7(a) and (b) show the PL intensity obtained from nano red of $Y_{1.936}O_3$:$Eu_{0.64}$ by feeding

the suspension precursor into RF plasma reactor. The host was micron-sized Y_2O_3 powders, and the exciter was $Eu(NO_3)_3$ salt. Plasma power was optimized for appropriate parameters. In this synthesis an enhanced PL intensity was obtained by controlling the plasma power from 30 to 50 kW. The higher the plasma power the better the PL intensity obtained. Besides, the PL intensity of red phosphor again was proved to be enhanced very much by doping Li appropriately as shown in Fig. 7(a) where excellent PL intensity was achieved by adding Li about 5 at.% into $Y_{1.936}O_3$:$Eu_{0.64}$. With this treatment the PL intensity showed the better quality compared to commercial red $Y_{1.936}O_3$:$Eu_{0.64}$ at least as far as intensity was concerned. The powder shape and size distributions were also fairly good compared to those of powders processed via dry precursors. The inset in Fig. 7(a) shows the excellent powder shape and size distribution that is achievable via suspension process.

Finally, nano red phosphor of Y_2O_3:Eu processed by feeding solution precursor was developed via aerosol nano synthesis. The precursors of $Y(NO_3)_3$ and $Eu(NO_3)_3$ salts were mixed and then fed into proprietary aerosol combustion nozzle as shown in Fig. 7(b). The figure shows the PL intensity obtained from the nano red synthesized by feeding the solution precursor. The average powder size was proved to be 20 nm, and the size distribution was uniform. The best PL intensity was obtained from the phosphor of Y_2O_3:$Eu_{0.15}$ which had slightly higher intensity at the wavelength of 615 nm compared to commercial red. Superior nano phosphor intensity was impossible for green or blue phosphors made from powder precursors. The processed nano red particles were found to coarsen slightly with the addition of Eu or Li over a certain amount. However, the growth rate was negligible.

4. Conclusion

In a radio-frequency plasma process, nanoparticles of phosphor are formed through recombination from vapor phases when a liquid or solid precursor is fed into a plasma reactor. When a solid type precursor is fed, local melting at the surface of the precursor also takes place during plasma reaction at the reactor. Whether a liquid or solid type precursor is used, the most important task is to improve crystallinity of targeted phosphor particles. Since crystallinity is influential on phosphor photoluminescence, a careful preparation process for each precursor's composition control, character, plasma process parameters, and post heat treatment must be developed in order for practical applications to have a sound economic basis. Nano synthesis of phosphors using liquid type precursors is promising if the production yield can be improved for commercial production. However, solid type precursors enable amore efficient process at the present stage of technology.

REFERENCES

1. M. I. Boulos, P. Fauchais, and E. Phender, "Thermal Plasmas:Fundamental and Applications," Vol. 1, pp33-47, Plenum Press, New York, 1994.
2. T. Ishigaki, "Synthesis of Ceramic Nanoparticles with Non-equillibrium Crystal Structure and Chemical Compositions by Controlled Plasma Process," *J. Ceram. Soc. Japan*, **116** 462-70 (2008).
3. Y. L. Li and T. Ishigaki, "Spherodization of Titanium Carbide Powders by Induction Thermal Plasma Processing," *J. Am. Ceram. Soc.*, **84** 1929-36 (2001).
4. T. Ishigaki, Y. L. Li, and E. Kadaoka, "Phase Formation and Microstructure of Titanium Oxides and Composites Produced by Thermal Plasma Oxidation of TiC," *J. Am. Ceram.*, **86** 1456-63 (2003).
5. Y. L. Li and T. Ishigaki, "Synthesis and Structural Characterization of Core-Shell Si-SiC Composite Particles by Thermal Plasma," *J. Ceram. Soc. Japan*, **115** 717-23 (2007).
6. N. Ohashi, T. Ishgaki, N. Okada, H. Taguchi, and H. Haneda, "Passivation of Active Recombination Centers in ZnO by Hydrogen Doping," *J. Appl. Phys.*, **93** [10] 6386-92 (2003).
7. N. Ohashi, T. Ishigaki, N. Okada, and H. Haneda, "Effect of Hydrogen Doping on Ultraviolet Emission Spectra of Various Types of ZnO," *Appl. Phys. Lett.*, **80** 2869-71 (2002).
8. C. J. Yang, S. D. Choi, E. B. Park, and Y. J. Lee, "Digest of Technical Paper of 7th IMID, SID," Vol. 7, pp. 1646-49, Book 2, Daegu, Korea, 2007.
9. T. Peng, H. Yang, X, Pu, Z. Jiang, and C. Yan, "Combustion Synthesis and Photoluminescence of $SrAl_2O_4$:Eu, Dy Phosphor Nanoparticles," *Materials Letters*, **58** 352-56 (2004).
11. Y. C. Kang, H. D. Park, and M. A. Lim, "Zn_2SiO_4:Mn Phosphor Particles Prepared by Spray Pyrolysis Process," *J. Information Display*, **2** [4] 57-62 (2001).
12. Private Communication with Dr. Young Joo Lee, Research Institute of Science & Technology, Nanotechnology Research Lab., Pohang, Korea, April 30.
13. A. N. Belsky and J. C. Krupa, "Luminescence Excitation Mechanisms of Rare Earth Doped Phosphors in the VUV Range," *Display*, **19** 185-96 (1999).